THE INFLUENCE OF VOIDS ON THE ENGINEERING CONSTANTS OF ORIENTED STRANDBOARD: A FINITE ELEMENT MODEL[1]

Qinglin Wu†
Associate Professor

Jong N. Lee†
Postdoctoral Researcher

and

Guangping Han
Visiting Research Associate
School of Renewable Natural Resources
Louisiana State University Agricultural Center
Baton Rouge, LA 70803

(Received September 2002)

ABSTRACT

A laminated model based on continuum theory combined with finite-element analysis (FEA) was used to predict the influence of voids on engineering constants of oriented strandboard (OSB). Cylindrical voids with three material density classes in the void region were considered at various void volume fractions (VVFs) and matrix anisotropies. It was found that the presence of voids resulted in substantial decreases in the elastic moduli and Poisson ratio of OSB. The hygroexpansion coefficients were affected little by voids. The elastic constants normalized with their void-free (matrix) values were found to depend little on the anisotropy of the matrix, especially at high VVFs. Increases of material density in the void region led to increases in predicted elastic constants. The predicted moduli values for the void models with certain material densities correlated well with available experimental data for the selected panel structures. The FEA provided a comprehensive numerical tool in predicting localized elastic properties of porous OSB. The model is the basis for modeling three-layer boards and for constructing in-plane modulus map of full-size panels.

Keywords: Finite element modeling, strand alignment level, in-plane elasticity, laminate model, linear expansion coefficient, structural strandboard, voids.

INTRODUCTION

The formation of an OSB mat from a suspension of resin-coated strands results in a relatively loosely packed mat. The density of the mat increases during the pressing operation, but the final product still contains a substantial volume occupied by voids. The void structure created by the interaction of raw material and mat formation parameters has many important implications for the evolution of the ultimate properties of the final product. In general, the presence of voids in OSB reduces its elastic moduli and influences its dimensional stability. Therefore, any micro-mechanical modeling of OSB would be incomplete unless attention is given to the void or pore structure of the product (Lenth and Kamke 1996).

Interest in predicting the consolidation behavior of wood strand mats has led to a significant inquiry of flake mat structure and its influence on panel properties. Suchsland (1962) investigated in-plane density variation, known as Horizontal Density Distribution (HDD), and determined that strand geometry affects the relative void volume in a mat.

[1] This (No: 02-40-0727) paper is published with the approval of the director of the Louisiana Agricultural Experiment Station.

† Member of SWST.

Wood and Fiber Science, 36(1), 2004, pp. 71–83

Suchsland and Xu (1989) continued the investigation to develop a model for the simulation of the HDD in flakeboard. From this research, it was concluded that both internal bond and thickness swelling properties were directly affected by HDD. Dai and Steiner (1994a, b) developed a probability-based model to describe randomly packed, short-fiber-type wood composites. The model uses the approach that the structural properties of a randomly formed strand network are random variables, essentially characterized by Poisson and exponential distributions, and predicts the distribution of the number of strand centers per unit of strand area, strand area coverage, free strand length, and void size (area as viewed from above). Lang and Wolcott (1996) developed a Monte Carlo simulation procedure that predicts the number of strands in the centroid of imaginary strand columns, the vertical distance between adjacent strands, and the position of the column centroid in relation to strand length based on data from laboratory-assembled mats. More recently, Lenth and Kamke (1996) developed a method for quantifying the cellular structure of a flakeboard mat. In their study, the mat structure was analyzed with respect to the percent area of the mat cross section occupied by voids, the size and shape of individual voids, and the distribution of void size and shape.

Analysis of the influence of the pore or void structures on effective mechanical and physical properties of flakeboard including OSB is extremely rare. Hunt and Suddarth (1974) developed a finite element model to predict tensile and shear moduli of mat-formed, homogeneous flakeboard as a function of the properties of its components and selected characteristics of the board. Strand orientations in the model were assigned according to a distribution function (random in the case of a board without directional properties). This early model analysis was quite limited where voids or other dislocations were not considered in their efforts to predict mechanical behavior. Shaler (1986) developed a modeling procedure to predict elastic moduli of OSB over a range of densities, resin levels, strand orientations, and species composition. The approach was based on the rule of mixture considering wood, resin, and air (void) inside the panel. It was shown that once the void volume is properly accounted, modulus of elasticity could be predicted reasonably well. However, strand alignment distribution parameters, and void shape and distribution were not considered implicitly in the model. Therefore, a new approach accounting for these important processing parameters is needed to advance current efforts in consolidation modeling of structural oriented strandboard to include effective engineering constants.

In an early study, a two-dimensional model to predict engineering constants of void-free OSB was developed using a continuum theory (Lee and Wu 2003). The orthotropic strand properties, strand alignment distribution, and panel shelling ratio for three-layer OSB were considered in the model. It was found that the laminate model is capable of predicting two-dimensional elastic moduli and linear expansion of OSB given the strand properties and strand alignment distributions. The orthotropy of the constituent matrix in OSB considerately increases the complexity of the micro-mechanical analysis of the influence of void on engineering constants of OSB, and no such analysis is readily available. The analysis of voids in an orthotropic matrix can, however, be based on a numerical solution of certain boundary-value problems. The finite element analysis (FEA) has been proven suitable for determining the effective mechanical properties of composite materials with regular packing and uniform size and shape of void inclusions (Adams and Doner 1967; Subramanian 1993).

The objectives of this study were 1) to develop a finite element model to quantify the effects of embedded voids (shape, size, volume, and material density) and matrix structure on elastic constants and moisture expansion coefficients of OSB; and 2) to verify the model prediction with available experimental data for the selected panel structures.

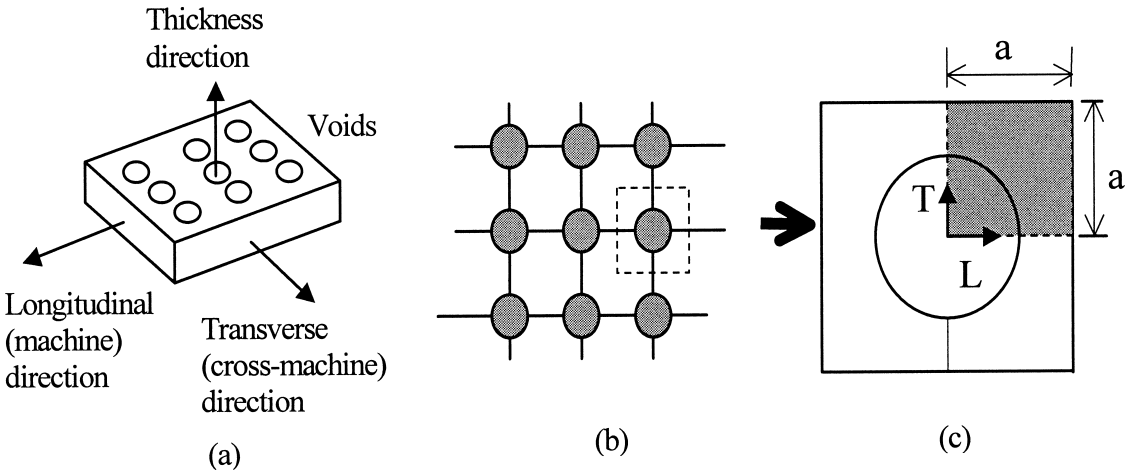

FIG. 1. Void models for OSB. a) Cylindrical through-thickness voids in OSB; b) Two-dimensional finite-element discretization of the RVE for cylindrical voids; c) Representative volume of the void model.

FINITE ELEMENT MODELING

Cylindrical void models

Modeling the mechanical response of porous OSB is complicated by the complexity of the panel structure. There are wide spectrums of size, shape, and relative orientation of the strands and void structure (Lenth and Kamke 1996). To develop tractable micro-mechanical solutions relating structural features and strand properties to the macroscopic behavior of OSB, idealized models have to be constructed and analyzed. While it is clear that the voids in OSB are not regular, a tractable numerical solution requires assumptions of uniform size and shape and regular packing of the voids. Modeling of local inelastic response of composite materials is sensitive to the details of the repeat void arrangement, but global (averaged) elastic properties are less sensitive to the packing geometry (Christensen and Lo 1979; Subramanian 1993).

It is assumed that the orthotropic matrix made of oriented wood strands with known strand alignment distribution and layering structure contains regularly spaced cylindrical voids (Fig. 1a). A two-dimensional discretization and a representative volume element (RVE) of the material are shown in Figs. 1b and 1c, respectively. Given the symmetries in geometry and loading, only ¼ of the RVE needs to be considered in the analysis. The L and T directions correspond to the longitudinal (machine) and transverse (cross-machine) directions, respectively. Three void configurations with different material densities in the void region (lower-left corner) were investigated (Fig. 2). Model 1 (Fig. 2a) contains a void with zero material density (a true void). Model 2 (Fig. 2b) contains voids with low (constant) material densities (compared with the solid region of the RVE). Model 3 (Fig. 2c) has a void with varying material densities, increasing from the center of the void zone to the matrix region. Strand alignment distribution and layering structure in the void region with non-zero material properties (Models 2 and 3) are assumed to be the same as the matrix. Four-nodded PLANE 42 quadrilateral plane stress elements (i.e., zero out-of-plane stresses) with two translation degrees of freedom at each node were employed (ANSYS 2002). A fine mesh is constructed near the void boundary to capture the steep stress and strain gradients and to investigate the mesh convergence.

Predicting engineering constants

Elastic moduli.—Elastic constants of a porous panel under the influence of various void

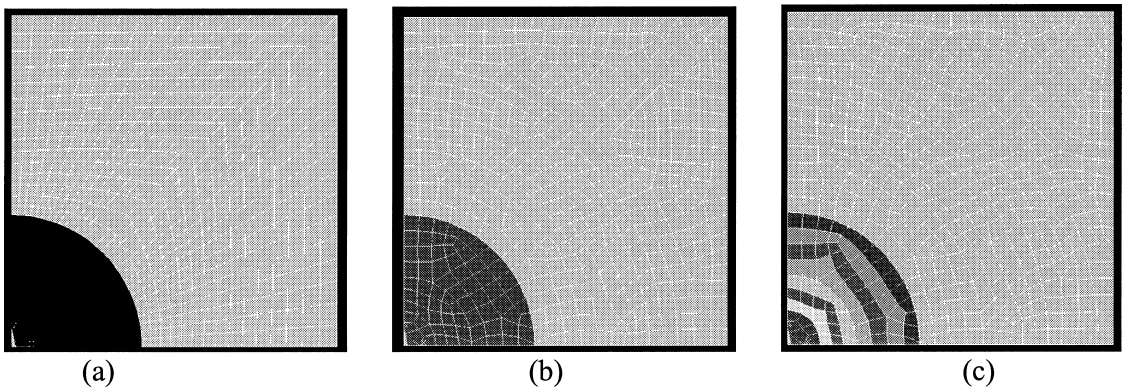

FIG. 2. Finite element models. a) Model 1—Zero void material density; b) Model 2—Low (constant) void material density; and c) Model 3—Varying void material density. The void region is represented by the lower-left corner and the rest of the RVE is matrix.

configurations were modeled by applying certain loading and boundary conditions to the RVE at a given void volume fraction (VVF = void volume/RVE volume). Tensile loading and boundary conditions imposed on the RVE are shown in Fig. 3a. A generalized plane strain (ϵ, mm/mm) analysis was performed by maintaining constant T-directional displacements of the nodes along the horizontal boundaries AE and BC of the RVE through coupled boundary conditions. The vertical boundaries DE and AB were also constrained to remain straight to generate compatibility with the neighboring RVEs after deformation. A uniform tensile stress (σ, MPa) was applied on the edge AB, and the displacements in the L and T directions, ΔL and ΔT, were computed. The effective elastic modulus, E_L (GPa), of the porous material was calculated as:

$$E_L = \sigma_L/\epsilon_L \quad \text{with} \quad \epsilon_L = \Delta L/a \qquad (1)$$

where, a is one side length of the RVE (cm,

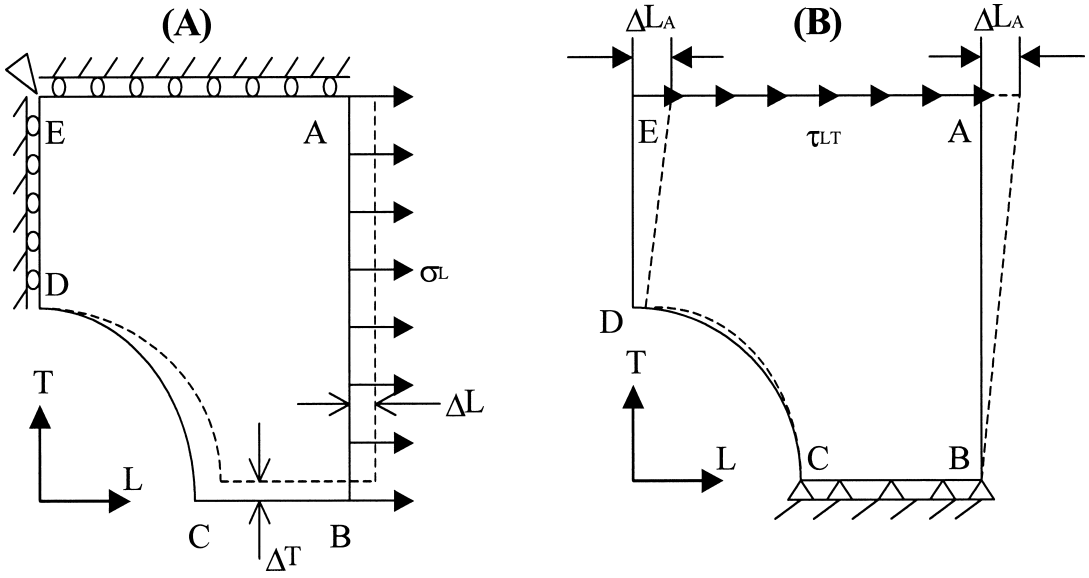

FIG. 3. Schematic of tensile (A) and shear (B) loading on the RVE containing voids.

TABLE 1. *Orthotropic engineering constants of solid OSB from the laminate model (Lee and Wu 2003) as input for the finite element analysis.*

Material Type	SAL[1] (%)	Density (g/cm^3)	Elastic Moduli (Gpa)		Shear Modulus (Gpa)[2]	Poisson Ratio	Swelling Coefficients (cm/cm/%MC)	
			E_{LM}	E_{TM}	G_{LTM}	ν_{LTM}	β_{LM}	β_{TM}
Matrix Region	80	0.7	11.77	0.454	1.586	0.190	0.000094	0.001633
	60	0.7	10.36	1.816	1.891	0.359	0.000170	0.000709
	<10	0.7	5.839	5.827	2.330	0.219	0.000357	0.000358
Void Region	Combined	0.1	1.150	0.046	2.380			
		0.2	2.560	0.099	2.195			
		0.3	4.089	0.164	2.040	0.190	0.000094	0.001633
		0.4	5.699	0.229	1.914			
		0.5	7.374	0.297	1.815			

[1] SAL—Strand alignment level in percent. The corresponding concentration parameter of the strand alignment distribution (K) is, respectively, 7, 2, and 0.15.
[2] Values of shear modulus in the void zone at various density levels were determined using Halpin-Tsai's micro-mechanics equation (Halpin and Tsai 1969; Jones 1975).

Fig. 1), and ϵ_L = tensile strain (cm/cm). Poisson's ratio, ν_{LT}, was calculated from

$$\nu_{LT} = -\Delta T/\Delta L \quad (2)$$

E_T was similarly computed by applying a stress σ_T (MPa) on the edge AE.

To represent shear loading on the RVE, a shear stress, τ_{LT} (MPa), was applied along the side AE (Fig. 3b). The side BC was constrained in the L and T directions, while the nodes on side AE were constrained to have uniform L- and T-directional displacements after deformation. To maintain the compatibility with the neighboring RVEs after shear deformation, the edges AB and DE of the RVE should remain straight and parallel. The L- and T-directional displacements of the nodes on side AB were thus constrained to vary linearly from 0 at B to their maximum values of Δ_A and ΔT_A at A. The effective in-plane shear modulus of the porous material, G_{LT} (MPa), was then calculated from the relation:

$$G_{LT} = \tau_{LT}/\gamma_{LT} \quad \text{with} \quad \gamma_{LT} = \Delta L_A/a \quad (3)$$

where, γ_{LT} is shear strain (cm/cm), and ΔL_A is the shear displacement (cm).

Moisture expansion coefficients.—To determine the influence of voids on the moisture expansion strain, the RVE was subjected to a moisture content increase (ΔMC, %) at all nodes. The nodes on the sides AB and BD were coupled in the L and T directions to maintain the compatibility with the neighboring RVEs. The resulting displacements in the L and T directions, ΔL and ΔT (cm), were computed. The moisture expansion strains, e_L and e_T (cm/cm), along the L and T directions were calculated as:

$$e_L = \Delta L/a \quad \text{and} \quad e_T/\Delta T/a \quad (4)$$

The moisture expansion coefficients along the two directions, β_L and β_T (cm/cm/%MC) were calculated as:

$$\beta_L = e_L/\Delta MC \quad \text{and} \quad \beta_T = e_T/\Delta MC \quad (5)$$

Model investigation

For each model, Young's moduli (E_{Lm} and E_{Tm}), shear modulus (G_{LTm}), Poisson ratio (ν_{LTm}), and hygroscopic expansion coefficients (β_{Lm} and β_{Tm}, cm/cm/%MC) of the matrix were generated by the laminate model from the previous work by Lee and Wu (2003) for each given board structure. The selected values of the properties are shown in Table 1. The length of the RVE side (a) was taken to be 1 cm. The density of the matrix was assumed to be 0.70 g/cm^3 for all three models. The power-form relationships between sample density and elastic moduli of OSB developed by Wu (1999) were used to estimate the elastic moduli of the material as a function of density. The equations have the following form:

$$E_L = 12.1314SG^{1.1589}\kappa^{0.1411} \qquad r^2 = 0.96$$

$$E_T = 3.6324SG^{1.1544}\kappa^{-0.2842} \qquad r^2 = 0.85 \quad (6)$$

where E_L and E_T are in GPa, SG is sample specific gravity, and κ is concentration parameter of the strand alignment distribution, which is directly related to the strand alignment level. Each model was run at six void volume fractions (i.e., 0.01, 0.03, 0.1, 0.3, 0.5, and 0.7). The void region in Model 1 had zero material density and property values. In Model 2, five material density levels (i.e., 0.1, 0.2, 0.3, 0.4, and 0.5 g/cm^3) in the void region were considered. In Model 3, material density in the void zone varied from 0.1 to 0.5 g/cm^3 at a rate of 0.05 g/cm^3/mm. The rate was estimated from the X-ray scanned density data of actual OSB samples machined from the single-layer, low density panels (i.e., density $\approx$ 0.45 g/cm^3). The samples contain large voids, which leads to localized in-plane density variation.

The predicted results were normalized with the modulus and Poisson ratio of the matrix without voids. The normalized constants were compared with analytical solutions for an isotropic matrix with true voids (Christensen and Lo 1979). To verify the model prediction with experimental data, mean density of each RVE was calculated considering material densities in both solid (matrix) and void regions as:

$$\rho_{RVE} = \rho_{Matrix} - VVF \cdot (\rho_{Matrix} - \rho_{Void}) \quad (7)$$

where ρ_{RVE} = mean density of the RVE (g/cm^3), ρ_{Matrix} = density of matrix (0.70 g/cm^3), and ρ_{Void} = density in the void region (g/cm^3). The predicted engineering constants from various void configurations were compared with available experimental data at various density levels (Wu 1999; Lee and Wu 2002).

RESULTS AND DISCUSSION

Predicted engineering constants

The predicted engineering constants from the three finite-element models for orthotropic RVEs containing cylindrical voids are summarized in Table 2. The data for boards at low alignment level (i.e., 60%) are plotted as a function of VVF in Fig. 4. Also shown in Fig. 4 are the data from the close form solution for a void-embedded isotropic matrix (Christensen and Lo 1979). The results were normalized with modulus and Poisson ratio of the material without voids.

The normalized E_L, E_T, and G_{LT} of OSB from Model 1 showed a similar trend as that of the analytical solution (Fig. 4). The finite element prediction of E_L and E_T are in good agreement with the analytical results at low VVFs. At higher VVFs, the finite element model predicted higher values of E_L and E_T than the analytical results (Figs. 4a and 4b). This may be related to the feature of self-consistent analytical models to underestimate the elastic stiffness at large volume fractions (Christensen and Lo 1979). The predicted shear modulus by Model 1 was smaller than the analytical results at low VVFs, as indicated by the gap between the two bottom curves in Fig. 4c. The gap narrowed down significantly as the VVF increased for the modulus, indicating a closer agreement between the two. The predicted Poisson ratios for OSB from Model 1 decreased as VVFs increased (Fig. 4d). The predicted values were significantly lower than these from the analytical solution at higher VVFs. The discrepancy may possibly be attributed to the regular phase geometry assumed in the finite element model. The Poisson ratio for porous materials is very sensitive to the phase geometry (Gibson and Ashby 1988). As a result, experimental data on Poisson ratio of porous materials show a large scatter around the value of the matrix. It is thus not recommended to correct the ratio for materials with voids.

Model 2 with a constant void material density of 0.3 g/cm^3 and Model 3 with void material density varying from 0.1 to 0.5 g/cm^3 predicted higher values of elastic moduli and Poisson ratios at a given VVF compared with results from Model 1 (Table 3). This indicates significant effects of material density in the void region on overall engineering properties of the RVE. Figure 4 shows significant difference of all four engineering constants predict-

TABLE 2. *Predicted engineering constants of OSB with two-dimensional cylindrical voids from the FE analyses.*[1,2]

VVF (%)	Model 1			Model 2			Model 3			Model 1			Model 2			Model 3		
	HA	LA	RA	HA	LA	RA	HA	LA	RA	HA	LA	RA	HA	LA	RA	HA	LA	RA
	Longitudinal Modulus (E_L, 1000 GPa)									Transverse Modulus (E_T, GPa)								
0	11.77	10.36	5.84	11.77	10.36	5.84	11.77	10.36	5.84	0.45	1.82	5.83	0.45	1.82	5.83	0.45	1.82	5.83
0.01	11.47	9.92	5.72	11.58	10.33	5.83	11.57	10.16	5.78	0.45	1.74	5.72	0.45	1.79	5.68	0.45	1.79	5.73
0.03	10.57	9.48	5.36	11.06	10.30	5.63	11.47	9.96	5.72	0.42	1.59	5.59	0.43	1.75	5.53	0.45	1.78	5.64
0.126	8.062	7.65	4.25	9.761	9.151	5.17	11.02	9.28	5.56	0.35	1.17	4.44	0.42	1.60	4.89	0.42	1.70	5.35
0.283	5.585	5.45	3.02	7.919	7.975	4.49	9.930	7.95	5.05	0.25	0.62	3.13	0.27	1.38	4.02	0.36	1.46	4.44
0.515	3.142	3.05	1.72	5.398	6.487	3.69	8.386	6.92	4.45	0.14	0.18	1.75	0.15	1.09	3.04	0.26	1.12	3.25
0.709	1.419	1.26	0.71	3.101	5.153	3.02	7.116	5.62	3.78	0.06	0.02	0.73	0.06	0.88	2.26	0.16	0.82	2.32
	Shear Modulus (G_{LT}, GPa)									Poisson Ratio (ν_{LT})								
0	1.59	1.89	2.33	1.59	1.89	2.33	1.59	1.89	2.33	0.19	0.35	0.22	0.19	0.36	0.22	0.19	0.36	0.22
0.01	1.48	1.75	2.16	1.49	1.78	2.31	1.55	1.84	2.27	0.19	0.33	0.21	0.18	0.36	0.22	0.19	0.35	0.22
0.03	1.23	1.64	2.05	1.37	1.57	2.29	1.51	1.79	2.22	0.19	0.28	0.19	0.18	0.36	0.22	0.19	0.34	0.22
0.126	0.83	1.13	1.44	1.19	1.51	2.24	1.39	1.76	2.18	0.18	0.21	0.15	0.18	0.35	0.23	0.19	0.31	0.22
0.283	0.59	0.79	1.02	1.00	1.52	2.21	1.22	1.72	2.16	0.15	0.13	0.09	0.17	0.34	0.24	0.19	0.26	0.23
0.515	0.18	0.26	0.35	0.74	1.49	2.11	0.94	1.65	2.15	0.11	0.06	0.04	0.16	0.34	0.25	0.18	0.24	0.24
0.709	0.02	0.03	0.04	0.53	1.33	1.92	0.65	1.59	2.08	0.07	0.13	0.11	0.17	0.34	0.28	0.17	0.20	0.25

[1] The void density for Model 2 was 0.3 g/cm^3. The void density for Model 3 varied from 0.1 to 0.5 g/cm^3. The density of solid region was 0.7 g/cm^3 for all three models.
[2] HA = high strand alignment level (80%), LA = low strand alignment level (60%) and RA = random strand alignment level (<10%).

TABLE 3. *Effect of void material density on the elastic properties of OSB predicted by Model 2 at the low alignment level (i.e., SAL ≈60%).*

Void Density (g/cm^3)	Void Volume Fraction						Void Volume Fraction					
	0	0.03	0.126	0.283	0.515	0.709	0	0.03	0.126	0.283	0.515	0.709
	Tensile Modulus (E_LGPa)						Transverse Modulus (E_T, GPa)					
0.0	10.36	7.703	5.991	4.264	2.451	1.002	1.816	1.606	1.249	0.889	0.511	0.209
0.1	10.36	9.639	8.231	6.772	4.571	2.830	1.816	1.707	1.461	1.118	0.734	0.437
0.2	10.36	9.835	8.777	7.345	5.604	4.025	1.816	1.732	1.535	1.252	0.916	0.658
0.3	10.36	10.30	9.151	7.975	6.487	5.153	1.816	1.753	1.601	1.375	1.096	0.876
0.4	10.36	10.08	9.500	8.602	7.407	6.336	1.816	1.771	1.660	1.489	1.269	1.091
0.5	10.36	10.16	9.782	9.146	8.264	7.480	1.816	1.786	1.711	1.594	1.435	1.302
	Shear Modulus (G_{LT}, GPa)						Poisson Ratio (ν_{LT})					
0.0	1.891	1.638	1.132	0.795	0.257	0.027	0.359	0.277	0.209	0.129	0.056	0.129
0.1	1.981	1.709	1.569	1.511	1.326	1.000	0.359	0.349	0.330	0.326	0.291	0.302
0.2	1.981	1.756	1.658	1.648	1.556	1.302	0.359	0.354	0.347	0.337	0.331	0.336
0.3	1.981	1.798	1.730	1.740	1.700	1.518	0.359	0.356	0.352	0.345	0.339	0.341
0.4	1.981	1.825	1.777	1.793	1.767	1.660	0.359	0.358	0.354	0.355	0.335	0.354
0.5	1.981	1.709	1.569	1.511	1.326	1.000	0.359	0.358	0.359	0.358	0.357	0.357

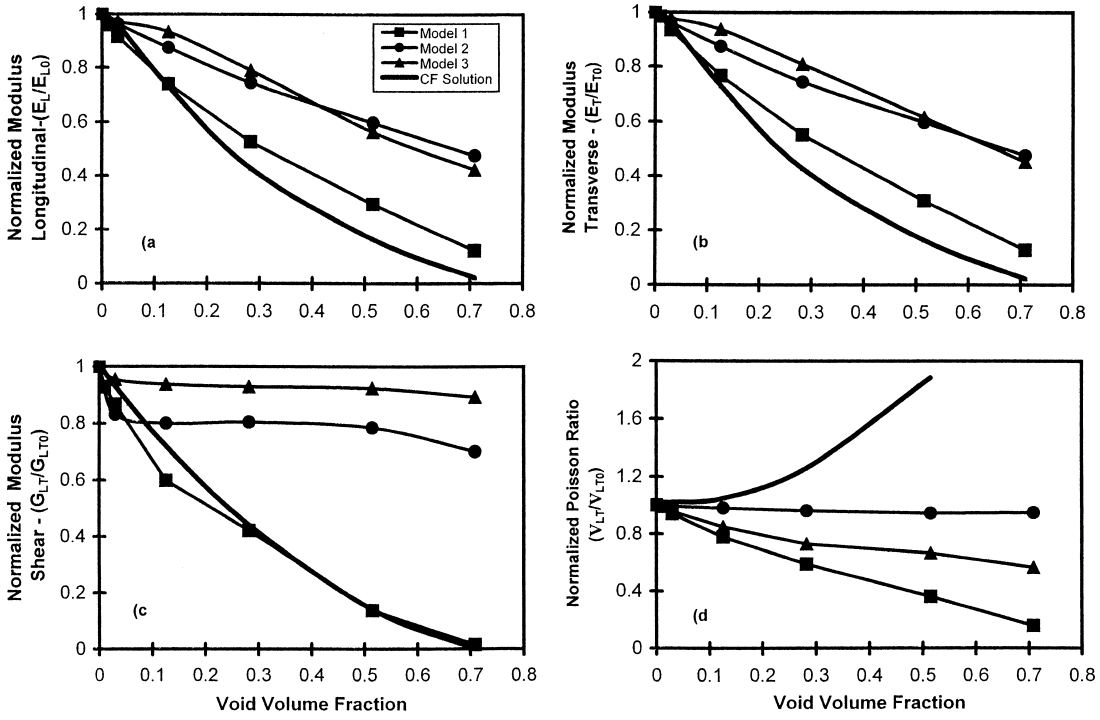

FIG. 4. Predicted engineering constants for single-layer porous OSB at the 80% strand alignment level. a) Longitudinal modulus, b) transverse modulus, c) shear modulus, and d) Poisson ratio. Data of the close-form (CF) solution are from Christensen and Lo (1975) for isotropic matrix. Model 1 had true voids (zero material density). The void density for Model 2 was 0.3 g/cm^3. The void density for Model 3 varied from 0.1 to 0.5 g/cm^3. The density of solid region was 0.7 g/cm^3 for all three models.

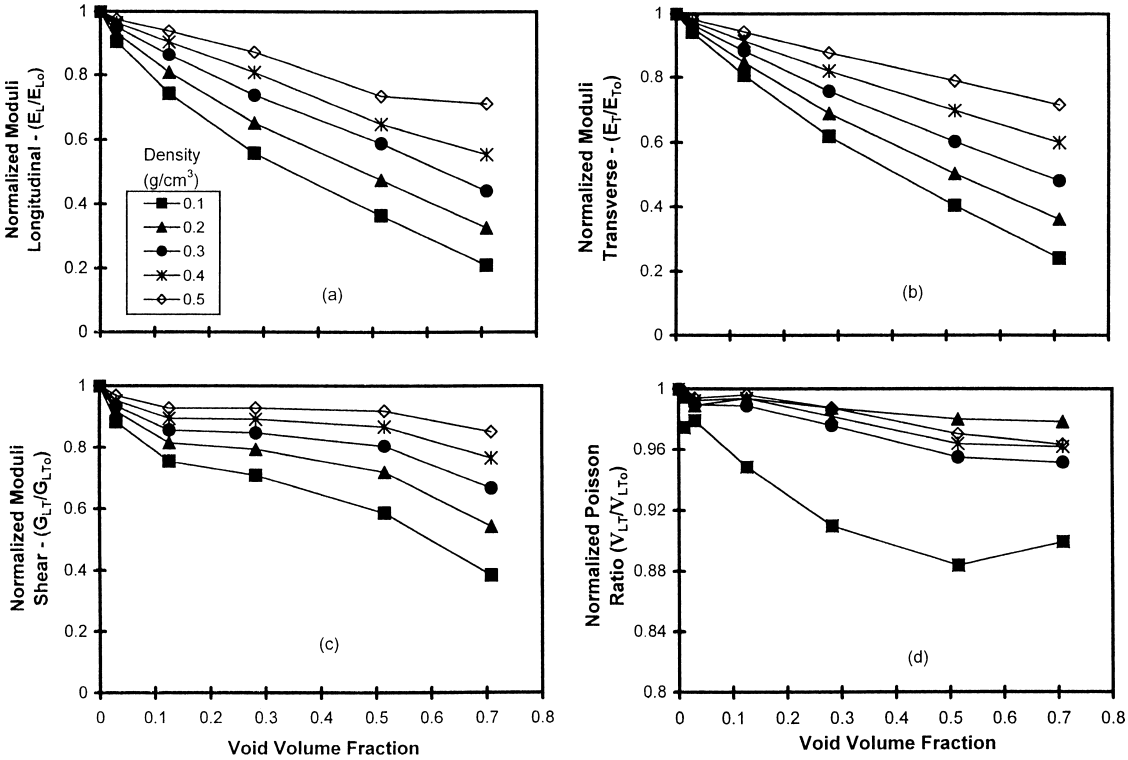

FIG. 5. Effect of material density in the void region on engineering constants of OSB predicted by Model 2. a) longitudinal modulus, b) transverse modulus, c) shear modulus, and d) Poisson ratio.

ed by the three models at various VVFs. The situations represented by Models 2 and 3 are more realistic for OSB. Because of the multilayer structure in OSB, a true void with zero material density does not exist in a given panel. However, there are low and high density areas throughout the panel.

The effect of void material density on the engineering constants of the RVE is further demonstrated in Fig. 5, which shows the predicted constants for boards with five void material densities (i.e., 0.1, 0.2, 0.3, 0.4, and 0.5 g/cm^3) at the 80% strand alignment level. As shown, all properties increased as the material density of the void increased. The normalized moduli and Poisson ratio gradually approached to one at all VVFs as the void material density reached the density value of the matrix. Therefore, a larger density contract between void and solid (matrix) regions led to lower overall engineering constants of the RVE. For a large panel of OSB, significant in-plane density variation would lead to a reduction of the engineering properties of the board. The rate of the density change in the void region as shown in Model 3 also played a role in controlling the overall RVE properties.

In general, matrix orthotropy had little influence on the engineering constants of the material in the presence of voids (Fig. 6—normalized moduli from the three void models). Both Models 1 and 2 predicted small and inconsistent variations of E_L and E_T among the three alignment levels at all VVFs. Thus, the effect of strand alignment level on the properties of OSB was overshadowed by the influence of the void for these two models. Model 3 predicted higher values of E_L and E_T for boards at high strand alignment levels and high VVFs.

There was also no significant influence of voids on in-plane hygroexpansion coefficients predicted by the finite element models along

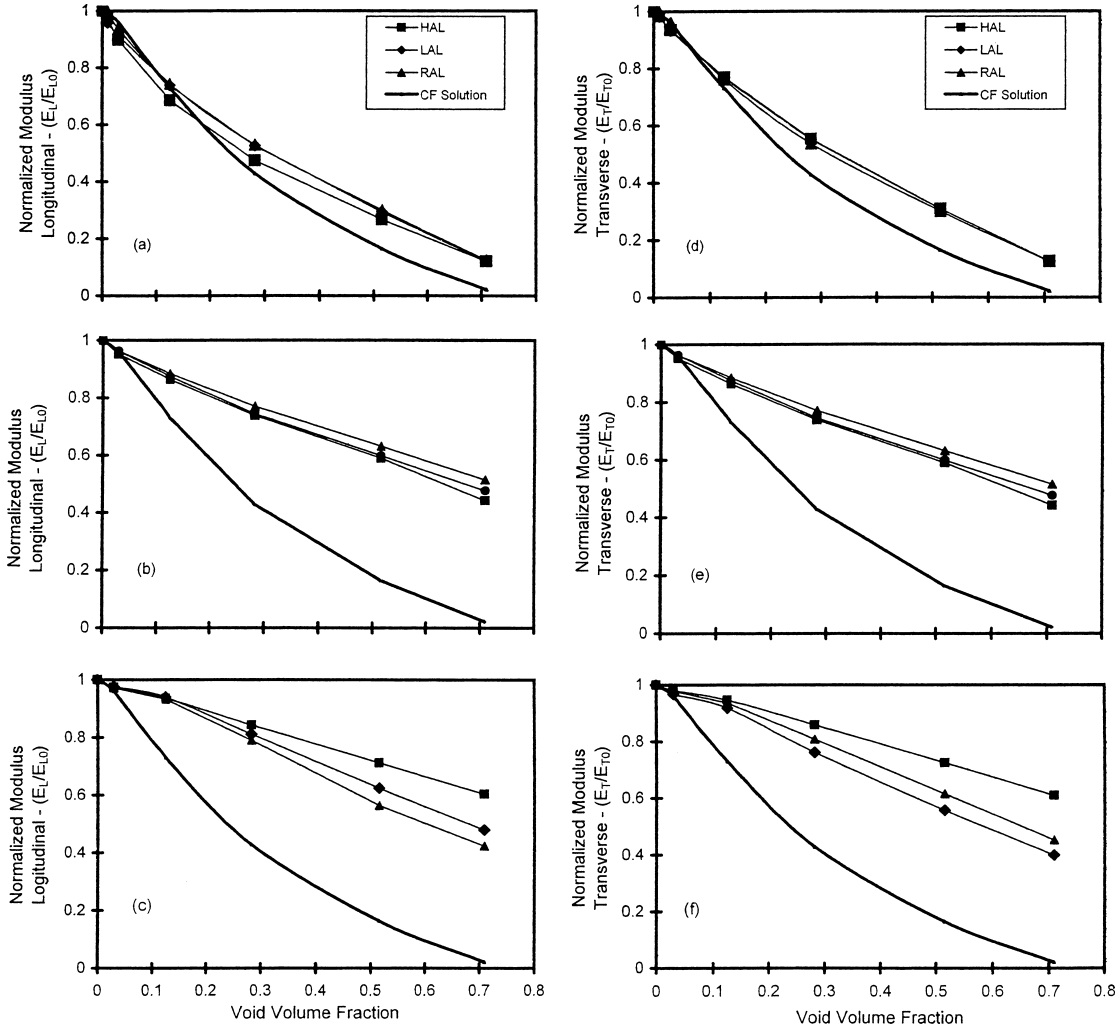

FIG. 6. Effect of strand alignment level of the engineering constant of OSB predicted by Model 1 (a, d), Model 2 (b, e) with a void material density of 0.3 g/cm^3, and Model 3 (c, f) with varying void material densities.

both longitudinal and transverse directions. Early experimental work on linear expansion (LE) of OSB as a function of density (Wu 1999) showed a slight increase of the longitudinal LE and a decrease of the transverse LE as panel density increased. The effect was attributed to cell-wall collapse during hot pressing, which is not reflected in the finite element model.

Model verification

A direct comparison of predicted longitudinal and transverse moduli with experimental data from Wu (1999) is shown in Fig. 7 for single-layer boards at three alignment levels. The experimental data and predicted results overlapped in the density region from 0.50 to 0.75 g/cm^3. There were more experimental data at the high density end and more predicted data at the low density end.

Within the overlapped density region, Model 1 with true voids predicted smaller modulus values compared with experimental data, especially along the transverse direction for boards at the high alignment level. This is so

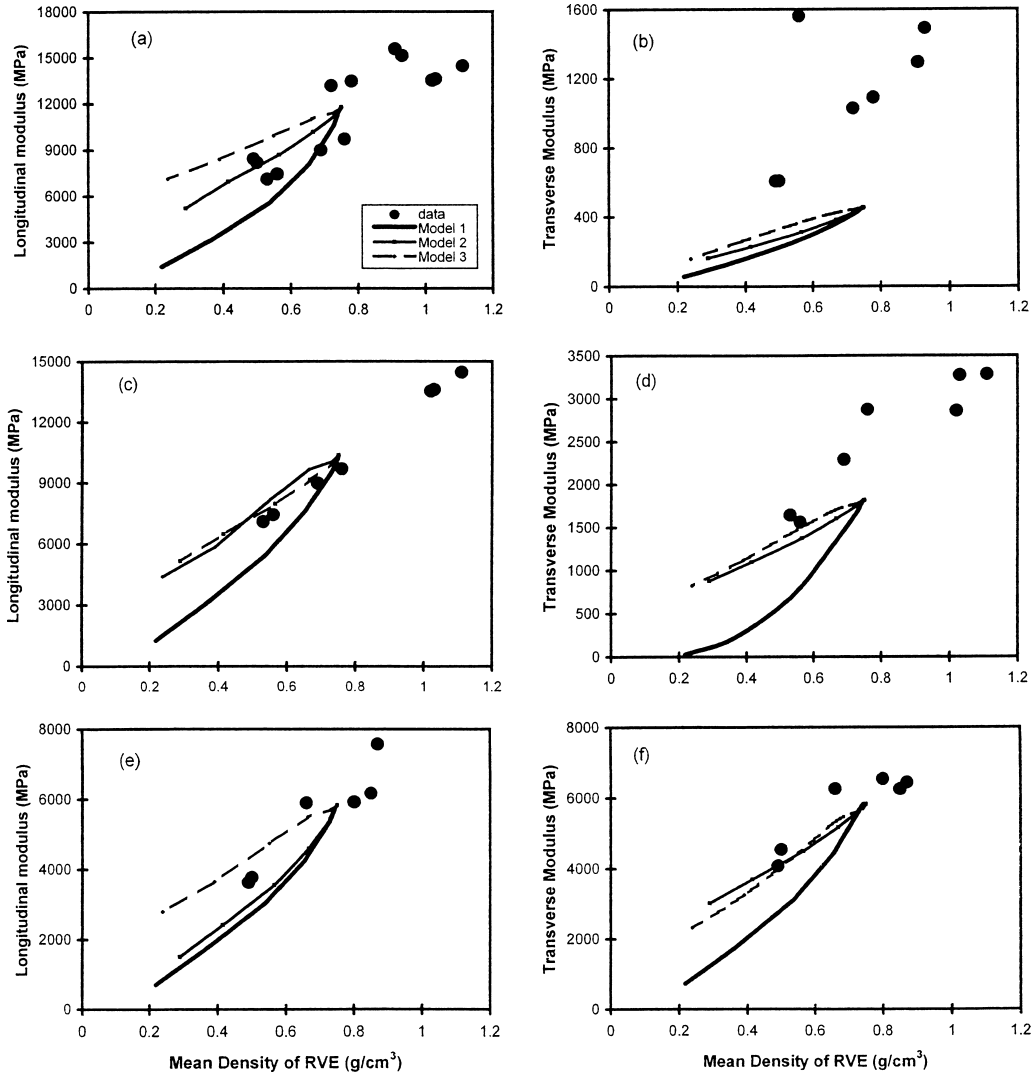

FIG. 7. Comparison of predicted longitudinal and transverse moduli from the three void models with experimental data from Wu (1999) for single-layer OSB at high (a and b), low (c and d), and random (e and f) alignment levels. Model 1 had true voids. The void density for Model 2 was 0.3 g/cm^3. The density in the void area for Model 3 varied from 0.1 to 0.5 g/cm^3. The density of solid region was 0.7 g/cm^3 for all three models.

because experimental panels did not contain true through-thickness voids (i.e., voids with zero material density) as those used in the model. As a result, the experimental elastic properties were higher, compared with the predicted values for similar panels. The experimental data of the transverse modulus for boards at the high alignment level were significantly larger than the predicted values by all three models. This was caused by very high E_L/E_T ratio (i.e., low E_T value) of the matrix for the panel group predicted by the laminate model (Lee and Wu 2003). The ANSYS program has limitations in dealing with materials with extremely high E_L/E_T ratios. The predictions by Model 2 (void material density = 0.3 g/cm^3) and Model 3 (void material density varied from 0.1 to 0.5 g/cm^3) showed a rea-

sonable agreement with the experimental data, especially for boards at low and random alignment levels. Thus, the accuracy of model prediction increased as the strand alignment level of the board decreased.

The slopes of the modulus and density curves predicted by Model 2 and Model 3 are in a general agreement with these of the experimental curves, except for the transverse modulus at the high alignment level (Fig. 7b). This indicated that the finite element model is capable of predicting the general trend of change of the elastic constants in OSB as a function of density with a proper account of the void material density and volume. There is a significant practical interest for lowering the density of OSB while maintaining its properties. The reduction of panel density will lead to increased void volume in the panel. The FEA shown in this paper can help establish threshold property values as the panel density is reduced (or increased as well) for various board structures.

CONCLUSIONS

A laminated model based on continuum theory was successfully combined with finite-element analysis to examine the influence of embedded voids on the engineering constants of OSB. Cylindrical voids with three void density configurations were considered for boards with different void volume fractions and matrix anisotropies. The presence of voids resulted in substantial decreases in the elastic moduli and Poisson ratio of OSB, while the hygroexpansion coefficients were affected little by voids. The normalized elastic constants were found to depend little on the anisotropy of the matrix, especially at high VVFs. Increases of the material density of the void region led to increases in predicted elastic constants. The predicted values for void models with certain material densities and VVFs correlated well with available experimental data. The model could be a useful tool for establishing threshold property values as the panel density is reduced or increased for various board structures. Future publications will deal with effects of void on the properties of the three-layer boards and constructing in-plane modulus map for full-size panels.

ACKNOWLEDGMENTS

This study was supported by the USDA National Research Initiative Competitive Grant Program (99-35103-8298). The financial contribution to the project is gratefully acknowledged.

REFERENCES

ADAMS, D. F., AND D. R. DONER. 1967. Transverse normal loading of a unidirectional composites. J. Composite Materials 1:152–164.

ANSYS. 2002. ANSYS 6.0 Online help. ANSYS Inc., Canonsburg, PA. www.ansys.com/service/documentation/index.htm.

CHRISTENSEN, R. M., AND K. H. LO. 1979. Solution for effective shear properties in three phase sphere and cylinder models. J. Mech. Phys. Solids 27:315–330.

DAI, C., AND P. R. STEINER. 1994a. Spatial structure of wood composites in relation to processing and performance characteristics. Part 2. Modeling and simulation of a randomly-formed strand layer network. Wood Sci. Technol. 28(2):135–146.

———, AND ———. 1994b. Spatial structure of wood composites in relation to processing and performance characteristics. Part 3. Modeling the formation of multilayered random strand mat. Wood Sci. Technol. 28(3): 229–239.

GIBSON, L. T., AND M. F. ASHBY. 1988. Cellular solid—structure and properties. Pergamon, New York, NY.

HALPIN, J. C., AND S. W. TASI. 1969. Effects of environmental factors on composite materials. AFML-TR 67-423.

HUNT, M. O., AND S. K. SUDDARTH. 1974. Prediction of elastic constants of particleboard. Forest Prod. J. 24(5): 52–57.

JONES, R. M. 1975. Mechanics of composite materials. McGraw-Hill, New York, NY. 355 pp.

LANG, E. M., AND M. P. WOLCOTT. 1996. A model for viscoelastic consolidation of wood-strand mats: Part I. Structural characterization of the mat via Monte Carlo simulation. Wood Fiber Sci. 28(1):100–109.

LEE, J. N., AND Q. WU. 2002. In-plane dimensional stability of three-layer oriented strandboard. Wood Fiber Sci. 34(1):77–95.

———, AND ———. 2003. Continuum modeling of engineering constants of oriented strandboard. Wood Fiber Sci. 35(1):24–40.

LENTH, C. A., AND F. A. KAMKE. 1996. Investigations of flakeboard mat consolidation. Part I. Characterizing the cellular structure. Wood Fiber Sci. 28(2):153–167.

SHALER, S. M. 1986. The usefulness of selected polymer

composite theories to predict the elastic moduli of orientated flakeboard. Ph.D. thesis, Pennsylvania State Uni., University Park, PA. 163 pp.

SUBRAMANIAN, L. 1993. Analysis of the influence of voids on the hygroelastic properties of paper. M.S. thesis, Dept. of Mechanical Engineering, Florida Atlantic University, Boca Raton, FL. 164 pp.

SUCHSLAND, O. 1962. The density distribution in flakeboard. Q. Bull., Michigan Agric. Experiment Station, Michigan State Univ. 45(1):104–121.

SUCHSLAND, O., AND H. XU. 1989. A simulation of the horizontal density distribution in a strandboard. Forest Prod. J. 39(5):29–33.

WU, Q. 1999. In-plane dimensional stability of oriented strandboard panel: Effect of processing variables. Wood Fiber Sci. 31(1):28–40.